DOI: http://dx.doi.org/10.12989/sem.2011.38.5.573

Nonlinear analysis of finite beam resting on Winkler foundation with consideration of beam-soil interface resistance effect

L. Zhang[1a], M.H. Zhao*[1], Y. Xiao[1,2b] and B.H. Ma[1a]

[1]*College of Civil Engineering, Hunan University, Changsha, 410082, China*
[2]*Department of Civil Engineering University of Southern California, Los Angeles, CA 90089-2531, USA*

(Received September 30, 2009, Accepted January 12, 2011)

Abstract. Comprehensive and accurate analysis of a finite foundation beam is a challenging engineering problem and an important subject in foundation design. One of the limitation of the traditional Winkler elastic foundation model is that the model neglects the effect of the interface resistance between the beam and the underneath foundation soil. By taking the beam-soil interface resistance into account, a deformation governing differential equation for a finite beam resting on the Winkler elastic foundation is developed. The coupling effect between vertical and horizontal displacements is also considered in the presented method. Using Galerkin method, semi-analytical solutions for vertical and horizontal displacements, axial force, shear force and bending moment of the beam under symmetric loads are presented. The influences of the interface resistance on the behavior of foundation beam are also investigated.

Keywords: foundation beam; Winkler model; deformation-coupling; interface resistance; nonlinear analysis; Galerkin method.

1. Introduction

Various engineering construction problems can be modeled as beams resting on elastic supports, so the theory for a beam on an elastic foundation is used widely in engineering, such as construction foundations, roadbed, railway and various pipelines (Ghosh and Madhav 1994, Cojocaru *et al.* 2003, Iimura 2004, Mallik *et al.* 2005, Zhang *et al.* 2009).

More recent work has been undertaken on the study of a beam on an elastic foundation from different aspects and many theoretical methods have been proposed (Aydogan 1995, Huang and Shi 1998, Onu 2000, Zhang and Murphy 2004, Hsu 2005, Ruge and Birk 2007, Sato *et al.* 2007, Fabijanic and Tambaca 2009, Kim 2009). The Winkler elastic foundation model and the Pasternak shearing model are the two simple foundation models used extensively to analyze the complicated beam-soil interaction problems. The Winkler elastic foundation model (Winkler 1867) is the one-

*Corresponding author, Professor, E-mail: mhzhaohd@21cn.com
[a]Ph.D Candidate
[b]Professor

parameter model based on pure bending beam theory. This model consists of infinitely many closely spaced but separate linear springs, has an advantage in obtaining fast solutions to the complicated structure-soil interaction problems, but has a limitation on representing the continuity of the soil deformation. The Pasternak shearing model (Pasternak 1954) is the two-parameter model based on the assumption of pure shear of the beam. In the Pasternak model, the interactions between the springs are considered, but no bending is taken into account and the vertical displacement of the beam is totally controlled by shear deformation.

Both the Winkler model and the Pasternak model do not consider the influences of interface resistance between beam and the soil below and the beam bending moment. However, recent studies demonstrate that the influence of this beam-soil interface resistance on the behavior of the beam should not be neglected. Tan (1997) proposed the partial solution of the infinite beam on elastic foundation with consideration of the effect of the interface resistance between the beam and the soil below. The study indicated that the interface resistance was indispensable when assess the response of the foundation beam under applied loads. Zhou and Du (2004) developed a modified Winkler foundation model by employing an individual elastic horizontal spring system into beam-soil interaction system. Zhao *et al.* (2008b) and Zhang *et al.* (2009) proposed power-series semi analytic solutions for a finite geocell reinforced beam on Winkler foundation with consideration of the effect of the horizontal resistance. On the assumption that no coupling effect was existed between horizontal and vertical displacements, Zhao *et al.* (2008a, 2009a) presented a fractional-steps method for a foundation beam with taking the influence of the beam-soil interface resistance into account. Furthermore, Yin (2000a, b) presented governing ordinary differential equations for a reinforced Timoshenko beam on an elastic foundation. An analytical solution for a reinforced beam subjected to a point load, closed solutions for the beam subjected to any pressure loading, and a particular solution for uniform pressure loading at any location of the beam were obtained. But among all the above methods, less attention is paid to consider the nonlinear deformation characteristic and vertical-horizontal coupling of deformation of the beam. Based on the Euler-Bernoulli theory with taking the geometric nonlinearity of the beam into account, Zhao *et al.* (2009b, c) proposed a method to assess of the behavior of an elastic foundation beam under various applied loads.

The purpose of this study is to show the beam-soil interface resistance effect on the behavior of a finite beam on an elastic foundation. A coupling governing differential equation in terms of beam deformation is established. The Galerkin method is introduced to obtain solutions for the internal forces and displacements of the beam subjected to symmetrical applied loads.

2. Basic equations

The analysis model of a finite beam resting on a Winkler elastic foundation with length l, width b, height h and elastic modulus E is illustrated in Fig. 1. The beam is subjected by symmetric loads including distributed loads q and concentrated loads P, The horizontal and vertical soil reactions q_x and q_z are expressed as

$$q_x = -k_x u$$
$$q_z = -k_z w \tag{1}$$

where k_x and k_z are the coefficients of horizontal and vertical soil reactions, respectively. Negative

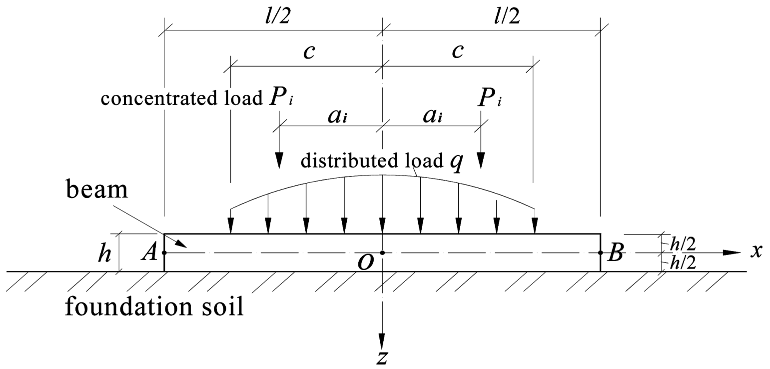

Fig. 1 Schematic illustration of foundation beam model

sign here implies that the direction of the force and the displacement is opposite.

Based on the basic hypothesis of the Euler-Bernoulli theory, the expressions of horizontal and vertical displacements u and w are as follows

$$w(x,z) = w^0(x)$$
$$u(x,z) = u^0(x) - z\frac{dw^0}{dx} \tag{2}$$

where $u^0(x)$ and $w^0(x)$ are the horizontal and vertical displacements on the neutral axis of beam, respectively.

Substituting Eq. (2) into Eq. (1), the expressions of q_x and q_z become

$$q_x = -k_x u = -k_x\left(u^0 - \frac{h}{2}\frac{dw^0}{dx}\right)$$
$$q_z = -k_z w^0 \tag{3}$$

By using the Euler-Bernoulli theory extending to problems involving moderately large rotations provided that the strain remains small, the horizontal strain ε_x of the beam is

$$\varepsilon_x(x,z) = \varepsilon_x^0 - z\frac{d^2w^0}{dx^2} = \left[\frac{du^0}{dx} + \frac{\chi}{2}\left(\frac{dw^0}{dx}\right)^2\right] - z\frac{d^2w^0}{dx^2} \tag{4}$$

where ε_x^0 is the strain on the neutral axis of beam; and χ is a nonlinear coefficient, if geometric nonlinearity of the beam is taken into account, $\chi = 1$, otherwise, $\chi = 0$.

For an elastic material, following relationship is existed

$$\sigma_x = E\varepsilon_x \tag{5}$$

where σ_x is the horizontal stress of beam.

Substituting Eq. (4) into Eq. (5) gives

$$\sigma_x = E\varepsilon_x = E\frac{du^0}{dx} - Ez\frac{d^2w^0}{dx^2} + \frac{\chi}{2}E\left(\frac{dw^0}{dx}\right)^2 \tag{6}$$

The relationships between the internal force and the stress at the cross section of the beam are

$$N = \int_A \sigma_x dA$$
$$M = \int_A \sigma_x z dA \tag{7}$$

where A is the cross-sectional area of beam; N is the axial force of beam with pulling force as positive; and M is the bending moment of beam.

Substituting Eq. (6) into Eq. (7) gives

$$N = EA\frac{du^0}{dx} + \frac{\chi}{2}EA\left(\frac{dw^0}{dx}\right)^2 - ES\frac{d^2w^0}{dx^2}$$
$$M = ES\frac{du^0}{dx} + \frac{\chi}{2}ES\left(\frac{dw^0}{dx}\right)^2 - EI\frac{d^2w^0}{dx^2} \tag{8}$$

where S and I are the static moment and inertia moment revolved around axis y, respectively. Since x-axis is a centroidal axis, so $S = 0$, then Eq. (8) can be reduced to

$$N = EA\frac{du^0}{dx} + \frac{\chi}{2}EA\left(\frac{dw^0}{dx}\right)^2$$
$$M = -EI\frac{d^2w^0}{dx^2} \tag{9}$$

All forces from the x-cross section to the right end of the beam are illustrated in Fig. 2. The relationship among the internal forces (such as axial force N, shear force Q and bending moment M) and external loads (such as distributed load q, concentrated load P, soil reactions q_x and q_z) are

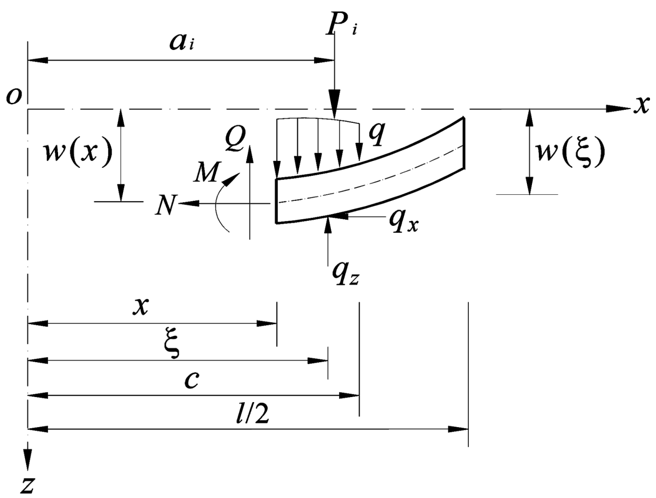

Fig. 2 Right part of the beam from x-cross section with all internal and external forces

shown as follows

$$N(x) = -\int_x^{l/2} k_x u^0(\xi) d\xi + \frac{h}{2} k_x \int_x^{l/2} \frac{dw^0(\xi)}{d\xi} d\xi$$

$$Q(x) = + \int_x^{l/2} [q(\xi) - k_z w^0(\xi)] d\xi + \sum P_i$$

$$M(x) = -\int_x^{l/2} \{[q(\xi) - k_z w^0(\xi)](\xi - x)\} d\xi - \sum P_i (a_i - x) - \int_x^{l/2} \left\{ k_x \left[u^0(\xi) - \frac{h}{2} \frac{dw^0(\xi)}{d\xi} \right] [h/2 - w^0(x) + w^0(\xi)] \right\} d\xi \tag{10}$$

Assuming that the displacements u^0 and w^0 own the following functions, respectively

$$u^0 = \sum_m U_m X_m(x)$$
$$w^0 = W_0 + \sum_m W_m Y_m(x) \tag{11}$$

where U_m, W_0 and W_m are the displacement vectors to be determined; and $X_m(x)$ and $Y_m(x)$ are displacement shape factors.

Substituting Eqs. (10) and (11) into Eq. (9) yields the governing differential equations of the beam as follows

$$EA \sum_m U_m \frac{dX_m(x)}{dx} + \frac{\chi}{2} EA \left(\sum_m W_m \frac{dY_m(x)}{dx} \right) \left(\sum_n W_n \frac{dY_n(x)}{dx} \right) = -k_x \int_x^{l/2} \left[\sum_m (U_m X_m(\xi)) \right] d\xi + \frac{hk_x}{2} \int_x^{l/2} \left[\sum_m \left(W_m \frac{dY_m(\xi)}{d\xi} \right) \right] d\xi \tag{12}$$

$$EI \sum_m W_m \frac{d^2 Y_m(x)}{dx^2} = \int_x^{l/2} [q(\xi)(\xi - x)] d\xi + \sum P_i (a_i - x) - k_z W_0 \int_x^{l/2} (\xi - x) d\xi - k_z \sum_m \left(W_m \int_x^{l/2} [Y_m(\xi)(\xi - x)] d\xi \right) +$$
$$\frac{hk_x}{2} \sum_m \left(U_m \int_x^{l/2} X_m(\xi) d\xi \right) - k_x \left(\sum_m [W_m Y_m(x)] \right) \left(\sum_n U_n \int_x^{l/2} X_n(\xi) d\xi \right) + k_x \int_x^{l/2} \left\{ \left(\sum_m [W_m Y_m(\xi)] \right) \left(\sum_n [U_n X_n(\xi)] \right) \right\} d\xi -$$
$$\frac{h^2 k_x}{4} \sum_m W_m \int_x^{l/2} \frac{dY_m(\xi)}{d\xi} d\xi + \frac{hk_x}{2} \sum_m W_m Y_m(x) \sum_n W_n \int_x^{l/2} \frac{dY_n(\xi)}{d\xi} d\xi - \frac{hk_x}{2} \int_x^{l/2} \left\{ \left(\sum_m [W_m Y_m(\xi)] \right) \left(\sum_n \left[W_n \frac{dY_n(\xi)}{d\xi} \right] \right) \right\} d\xi \tag{13}$$

Substituting the second equation in Eq. (11) into the second equation in Eq. (10) and considering force equilibrium in z direction, the following equation can be obtained

$$\int_0^{l/2} \left\{ q(\xi) - k_z \left[W_0 + \sum_m (W_m Y_m(\xi)) \right] \right\} d\xi + \sum P_i = 0 \tag{14}$$

Eqs. (12) to (14) are the basic governing equations of the beam in the terms of displacement functions.

3. Boundary and continue conditions

According to the symmetry, the horizontal displacement u^0 and rotation angle θ ($\theta = dw^0/dx$) at the mid point $x = 0$ are both zero. In this study, only the beam with free-ends is considered, so the axial force N and bending moment M at the beam right end $x = l/2$ are both zero too. Then, the following boundary conditions are existed

$$\begin{cases} u^0\big|_{x=0} = 0 \\ \theta\big|_{x=0} = 0 \\ Q\big|_{x=0} = -P_0/2 \end{cases} \quad \text{and} \quad \begin{cases} N\big|_{x=l/2} = 0 \\ M\big|_{x=l/2} = 0 \\ Q\big|_{x=l/2} = P_l \end{cases} \tag{15}$$

where P_0 and P_l are the concentrated loads acting at the points $x = 0$ and $x = l/2$, respectively. If there is no concentrated load acting at any of these two points, the corresponding concentrated load is zero. For example, if there is no concentrated load at the point $x = 0$, then, $P_0 = 0$.

Based on the concept of Euler-Bernoulli theory, the deformation of the beam at every point is continuing.

4. Solutions of equations

4.1 Assumptions of shape functions

In order to get higher calculation accuracy, the displacement shape factors $X_m(x)$ and $Y_m(x)$ are assumed to be expressed by a function combined with hyperbolic functions and trigonometric functions as shown below

$$\begin{aligned} X_m(x) &= \frac{\sinh\alpha_m x}{\sinh(\alpha_m l/2)} - \frac{\sin\alpha_m x}{\sin(\alpha_m l/2)} \\ Y_m(x) &= \frac{\cosh\beta_m x}{\cosh(\beta_m l/2)} + \frac{\cos\beta_m x}{\sin(\beta_m l/2)} \end{aligned} \tag{16}$$

where α_m and β_m are the undetermined coefficients. As the trial functions in Eq. (11) should satisfy the above boundary and continuity conditions, the following transcendental equation can be obtained

$$\coth\lambda_m - \cot\lambda_m = 0 \tag{17}$$

where

$$\lambda_m = \alpha_m l/2 = \beta_m l/2 \tag{18}$$

An approximate solution of Eq. (17) is given below

$$\lambda_m = \pi(m + 0.25) \tag{19}$$

4.2 Solutions of equations by using Galerkin method

First of all, Eqs. (12), (13) and (14) are rewritten as follows

$$EA\sum_m U_m \frac{dX_m(x)}{dx} + k_x \int_x^{l/2}\left(\sum_m U_m X_m(\xi)\right) d\xi - \frac{hk_x}{2}\int_x^{l/2}\left(\sum_m W_m \frac{dY_m(\xi)}{dx}\right) d\xi +$$
$$\frac{\chi}{2} EA\left(\sum_m W_m \frac{dY_m(x)}{dx}\right)\left(\sum_n W_n \frac{dY_n(x)}{dx}\right) = 0 \tag{20}$$

$$-\frac{hk_x}{2}\sum_m\left(U_m \int_x^{l/2} X_m(\xi)d\xi\right) + k_z W_0 \int_x^{l/2}(\xi - x)d\xi + EI\sum_m W_m \frac{d^2Y_m(x)}{dx^2} + k_z \sum_m\left(W_m \int_x^{l/2}[Y_m(\xi)(\xi - x)]d\xi\right) +$$
$$k_x\left(\sum_m [W_m Y_m(x)]\right)\left(\sum_n U_n \int_x^{l/2} X_n(\xi)d\xi\right) - k_x \int_x^{l/2}\left\{\left(\sum_m [W_m Y_m(\xi)]\right)\left(\sum_n [U_n X_n(\xi)]\right)\right\}d\xi + \frac{h^2k_x}{4}\sum_m W_m \int_x^{l/2}\frac{dY_m(\xi)}{d\xi}d\xi -$$
$$\frac{hk_x}{2}\sum_m W_m Y_m(x)\sum_n W_n \int_x^{l/2}\frac{dY_n(\xi)}{d\xi}d\xi + \frac{hk_x}{2}\int_x^{l/2}\left\{\left(\sum_m [W_m Y_m(\xi)]\right)\left(\sum_n\left[W_n \frac{dY_n(\xi)}{d\xi}\right]\right)\right\}d\xi$$
$$= \int_x^{l/2}[q(\xi)(\xi - x)]d\xi + \sum P_i(a_i - x) \tag{21}$$

$$k_z W_0 \frac{l}{2} + k_z \sum_m W_m \int_0^{l/2} Y_m(\xi)d\xi = \int_0^{l/2} q(\xi)d\xi + \sum P_i \tag{22}$$

It is observed that Eqs. (20) to (22) are too complex to solve directly. The Galerkin method is employed herein to solve this equation system. And the *k*th step of the Galerkin method is introduced as follows.

(1) Multiplying every term in Eq. (20) by the primary function $X_i(x)$, and integrating in the range of $0 < x < l/2$, the following matrix expression can be obtained

$$\mathbf{B}\{U\} + \mathbf{C}^{(k)}\{W\} = \mathbf{0} \tag{23}$$

where, $\{U\}$ and $\{W\}$ are $m \times 1$ matrices; $\mathbf{B}$ and $\mathbf{C}^{(k)}$ are $m \times m$ matrices with elements shown below

$$B_{im} = B_{im}^{(a)} + B_{im}^{(b)}$$
$$C_{im}^{(k)} = C_{im}^{(a)} + C_{im}^{(b,k)} \tag{24}$$

where

$$B_{im}^{(a)} = EA\int_0^{l/2}\left(X_i(x)\frac{dX_m(x)}{dx}\right)dx$$
$$B_{im}^{(b)} = k_x \int_0^{l/2}\left\{\left[\int_x^{l/2} X_m(\xi)d\xi\right]X_i(x)\right\}dx \tag{25}$$
$$C_{im}^{(a)} = -\frac{hk_x}{2}\int_0^{l/2}\left[\left(\int_x^{l/2}\frac{dY_m(\xi)}{d\xi}d\xi\right)X_i(x)\right]dx$$
$$C_{im}^{(b,k)} = \frac{\chi}{2}EA\int_0^{l/2}\left[\left(\sum_n W_n^{(k-1)}\frac{dY_n(x)}{dx}\right)\frac{dY_m(x)}{dx}X_i(x)\right]dx \tag{26}$$

The superscript (k) in $\mathbf{C}^{(k)}$, $C_{im}^{(k)}$ and $C_{im}^{(b,k)}$ means these matrixes or matrix elements are obtained in the kth iteration step; the superscript "$(k-1)$" in $W_n^{(k-1)}$, which is a part of the integrand function in second equation in Eq. (26), means the value of W_n can be obtained in the previous (k-1)th iteration step.

(2) Multiplying every term in Eq. (21) by the other primary function $Y_i(x)$ and integrating in $0<x<l/2$, the following matrix expression can be obtained

$$\mathbf{T}\{U\}+W_0\mathbf{g}+\mathbf{R}^{(k)}\{W\} = \mathbf{d} \tag{27}$$

where, **g** and **d** are $m\times 1$ matrices; **T** and $\mathbf{R}^{(k)}$ are $m\times m$ matrices; elements in **g**, **d**, **T** and $\mathbf{R}^{(k)}$ are

$$g_i = k_z \int_0^{l/2}\left[\left(\int_x^{l/2}(\xi-x)d\xi\right)Y_i(x)\right]dx$$

$$d_i = \int_0^{l/2}\left\{\left(\int_x^{l/2}\left[q(\xi)(\xi-x)\right]d\xi+\sum P_i(a_i-x)\right)Y_i(x)\right\}dx$$

$$T_{im} = -\frac{hk_x}{2}\int_0^{l/2}\left[\left(\int_x^{l/2}X_m(\xi)dx\right)Y_i(x)\right]d\xi$$

$$R_{im}^{(k)} = R_{im}^{(a)}+R_{im}^{(b)}+R_{im}^{(c)}+R_{im}^{(d,k)}+R_{im}^{(e,k)}+R_{im}^{(f,k)}+R_{im}^{(g,k)} \tag{28}$$

where

$$R_{im}^{(a)} = EI\int_0^{l/2}\left[Y_i(x)\frac{d^2Y_m(x)}{dx^2}\right]dx$$

$$R_{im}^{(b)} = k_z\int_0^{l/2}\left[\left(\int_x^{l/2}Y_m(\xi)(\xi-x)d\xi\right)Y_i(x)\right]dx$$

$$R_{im}^{(c)} = \frac{h^2k_x}{4}\int_0^{l/2}\left[\left(\int_x^{l/2}\frac{dY_m(\xi)}{d\xi}d\xi\right)Y_i(x)\right]dx$$

$$R_{im}^{(d)} = k_x\int_0^{l/2}\left\{Y_m(x)\left(\sum_n U_n^{(k-1)}\int_x^{l/2}X_n(\xi)d\xi\right)Y_i(x)\right\}dx$$

$$R_{im}^{(e,k)} = -k_x\int_0^{l/2}\left\{\left\{\int_x^{l/2}\left[Y_m(\xi)\left(\sum_n U_n^{(k-1)}X_n(\xi)\right)\right]d\xi\right\}Y_i(x)\right\}dx$$

$$R_{im}^{(f,k)} = -\frac{hk_x}{2}\int_0^{l/2}\left[\left(Y_m(x)\sum_n W_n^{(k-1)}\int_x^{l/2}\frac{dY_n(\xi)}{d\xi}d\xi\right)Y_i(x)\right]dx$$

$$R_{im}^{(g,k)} = \frac{hk_x}{2}\int_0^{l/2}\left\{\left\{\int_x^{l/2}\left[\left(Y_m(\xi)\sum_n\left(W_n^{(k-1)}\frac{dY_n(\xi)}{d\xi}\right)\right)d\xi\right]\right\}Y_i(x)\right\}dx \tag{29}$$

The superscripts (k) and $(k-1)$ have the same meanings as explained above.

(3) Transforming Eq. (22) into

$$DW_0 + \mathbf{H}^T\{W\} = F \tag{30}$$

where $\boldsymbol{H}$ is a $m \times 1$ matrix with element $H_i = k_z \int_0^{l/2} Y_i(\xi)d\xi$; and

$$D = k_z l/2$$

$$F = \int_0^{l/2} q(\xi)d\xi + \sum P_i \tag{31}$$

Combining with Eqs. (23), (27) and (30), the following system with $2m + 1$ equations in the kth iterative step is derived

$$\begin{bmatrix} B_{11} & \cdots & B_{1m} & 0 & C_{11}^k & \cdots & C_{1m}^k \\ \vdots & \ddots & \vdots & \vdots & \vdots & \ddots & \vdots \\ B_{m1} & \cdots & B_{mm} & 0 & C_{m1}^k & \cdots & C_{mm}^k \\ T_{11} & \cdots & T_{1m} & g_1 & R_{11}^k & \cdots & R_{1m}^k \\ \vdots & \ddots & \vdots & \vdots & \vdots & \ddots & \vdots \\ T_{m1} & \cdots & T_{mm} & g_m & R_{m1}^k & \cdots & R_{mm}^k \\ 0 & \cdots & 0 & D & H_1 & \cdots & H_m \end{bmatrix} \begin{Bmatrix} U_1^k \\ \vdots \\ U_m^k \\ W_0^k \\ W_1^k \\ \vdots \\ W_m^k \end{Bmatrix} = \begin{bmatrix} 0 \\ \vdots \\ 0 \\ d_1 \\ \vdots \\ d_m \\ F \end{bmatrix} \tag{32}$$

The elements in the above matrix equation with the superscript (k) means the values of these elements should be regenerate in every iterative step, while the other elements without the superscript (k) means the values of these elements remain constant in every iterative step.

Then the $2m+1$ numbers of undetermined coefficients as $U_1, U_2, \ldots, U_m, W_0, W_1, W_2, \ldots, W_m$ can be determined by the above equations set Eq. (32). The detailed iterative step to obtain $U_1, U_2, \ldots, U_m, W_0, W_1, W_2, \ldots, W_m$ through solving the nonlinear equations set Eq. (32) is introduced as follows:

(1) In the first iterative step, $k = 1$. Assuming $\{U^{(k-1=0)}\}$ in $R_{im}^{(e,k=1)}$(shown in Eq. (29)) and $\{W^{(k-1=0)}\}$ in $C_{im}^{(b,k=0)}$, $R_{im}^{(f,k=1)}$ and $R_{im}^{(g,k=1)}$ (shown in Eqs. (26) and (29), respectively) are zero, and substituting $C_{im}^{(b,k=1)}$, $R_{im}^{(e,k=1)}$, $R_{im}^{(f,k=1)}$ and $R_{im}^{(g,k=1)}$ with $\{U^{(k-1=0)}\} = 0$ and $\{W^{(k-1=0)}\} = 0$ into Eqs. (24) and (28) obtains $C_{im}^{(k=1)}$ and $R_{im}^{(k=1)}$, respectively. Then substituting $C_{im}^{(k=1)}$ and $R_{im}^{(k=1)}$ into Eq. (32) and solving Eq. (32), obtains $U_1, U_2, \ldots, U_m, W_0, W_1, W_2, \ldots, W_m$ in the first iterative step, and designates them as $\{U^{(1)}\}$, $W_0^{(1)}$ and $\{W^{(1)}\}$.

(2) In the second iteration step, $k = 2$, substituting $(k-1) = 1$, $\{U^{(1)}\}$, $W_0^{(1)}$ and $\{W^{(1)}\}$ into Eqs.(26) and (29) obtains $C_{im}^{(b,k=2)}, R_{im}^{(e,k=2)}, R_{im}^{(f,k=2)}$ and $R_{im}^{(g,k=2)}$. Then substituting $C_{im}^{(b,k=2)}$, $R_{im}^{(e,k=2)}$, $R_{im}^{(f,k=2)}$ and $R_{im}^{(g,k=2)}$ into Eqs. (24) and (28) obtains $C_{im}^{(k=2)}$ and $R_{im}^{(k=2)}$. Solving Eq. (32) with $C_{im}^{(k=2)}$ and $R_{im}^{(k=2)}$, obtains $\{U^{(2)}\}$, $W_0^{(2)}$ and $\{W^{(2)}\}$ in the second iteration step.

(3) The rest may be deduced by analogy, until the following inequalities

$$\frac{\left\|(\{U^{(k)}\}-\{U^{(k-1)}\})^T(\{U^{(k)}\}-\{U^{(k-1)}\})\right\|}{\left\|\{U^{(k)}\}^T\{U^{(k)}\}\right\|}<\zeta$$

$$\frac{\left\|(\{W^{(k)}\}-\{W^{(k-1)}\})^T(\{W^{(k)}\}-\{W^{(k-1)}\})\right\|}{\left\|\{W^{(k)}\}^T\{W^{(k)}\}\right\|}<\zeta$$

$$\frac{\left\|(W_0^{(k)})-W_0^{(k-1)}\right\|}{(W_0^{(k)})}<\zeta \tag{33}$$

are satisfied, where ζ is an assumed convergence error.

If in the kth step, the above inequalities set (33) are satisfied, then, $\{U^{(k)}\}$, $W_0^{(k)}$ and $\{W^{(k)}\}$ are the desired values.

5. Calculation of deformations and internal forces

Substituting U_1, U_2, $\cdots$, U_m, W_0, W_1, W_2, $\cdots$, and W_m from the matrices $\{U^{(k)}\}$, $\{W_0^{(k)}\}$ and $\{W^{(k)}\}$ into Eq. (11), the displacements $u^0(x, z)$ and $w^0(x)$ of beam can be obtained. Substituting these displacements into Eq. (2), the displacements at any point of the beam can be obtained. Then, substituting the expressions of $u^0(x, z)$ and $w^0(x)$ into Eq. (10), the internal forces including the axial force, N, shear force, Q, and bending moment, M, at any cross-section of beam can be obtained.

A computer program based on the above equations has been developed to obtain the final solutions.

6. Numerical validation of analysis

6.1 Case 1

In order to validate the solutions proposed in this paper, the same beam shown in Fig. 3 and analyzed by a finite element method (FEM) proposed by Ma and Ai (2002) were employed herein. The detailed information about the FEM in Ma and Ai's study can be found in Appendix A. The analysis foundation beam is 29.0 m long, 3.0 m wide, 1.0 m high, and the other parameters were chosen to be the same as those in Ma and Ai's study and they are: flexural rigidity $EI = 5.125 \times 10^6$ kN·m^2; horizontal coefficients of foundation reaction $k_x = 7.5 \times 10^3$ kN/m^3; and vertical coefficients of foundation reaction $k_z = 5 \times 10^3$ kN/m^3. In the performed numerical computations of current method, to minimize the numerical errors, a convergence study has been carried out and it has been observed that the results converge for the number of displacement vectors, m, equal to or greater than 10. When m increases from 10 to 11, the maximum difference of the approximation results is less than 10^{-3}, which can be accepted by engineers. Hence, in the following studies the number of vectors, m, has been taken as 11. The comparisons of nodes deformations, shear forces and moments derived from the present method with those from the FEM (Ma and Ai 2002) are shown in Figs. 4-6. The results also compared with those obtained from the classical method for the elastic

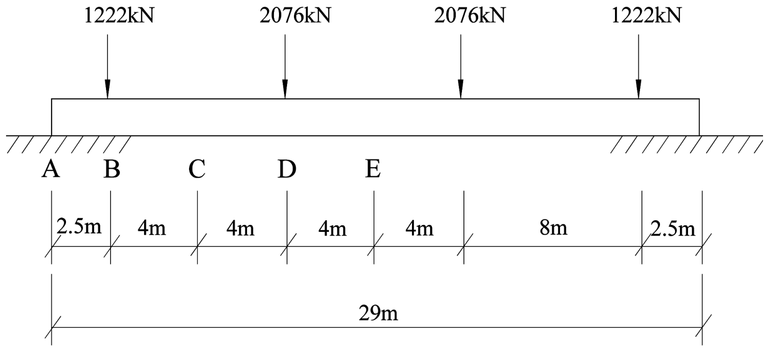

Fig. 3 Elastic foundation beam with loads on it

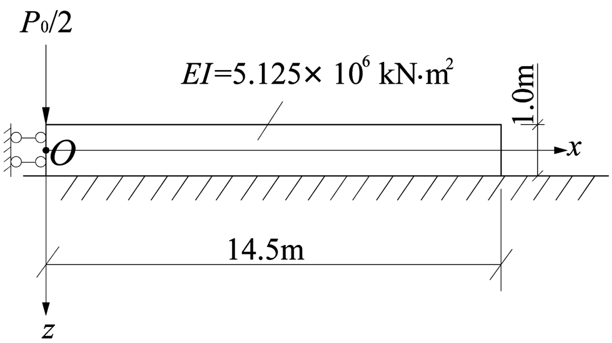

Fig. 4 Right half of a foundation beam under a concentrated load in the mid-span

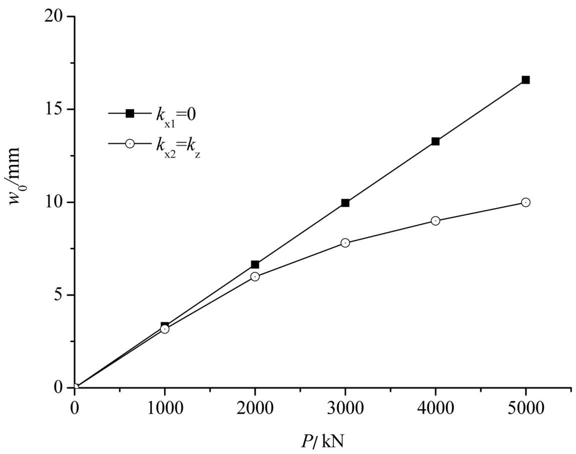

Fig. 5 Relationship between P and w_0

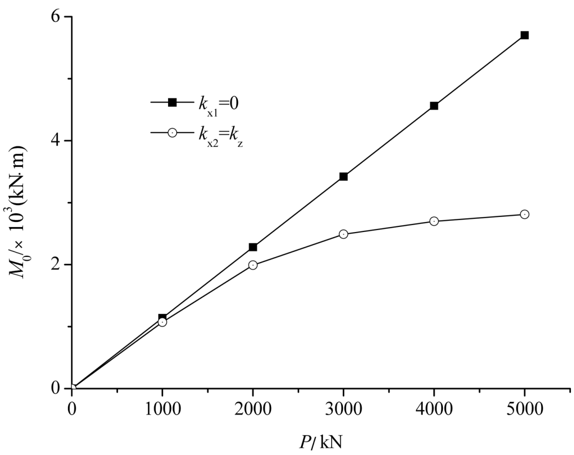

Fig. 6 Relationship between P and M_0

beam on Winkler foundation (Long 1981, shown in Appendix B).

From Tables 1-3, it is obvious that when the beam-soil interface resistance is not taken into account, the results obtained from the present method are much closer to the results from the classical method (Long 1981) for the beam on elastic foundation, than the results obtained from the FEM proposed by Ma and Ai (2002). That is because the FEM (Ma and Ai 2002) derived from the

Table 1 Comparison of node deformations with existing methods /mm

Calculation methods		A	B	C	D	E
without resistance	Long's method/w_1	12.84	13.62	14.69	16.76	16.79
	Ma's method/w_2	13.16	13.66	13.60	18.02	16.65
	Present method/w_3	12.95	13.67	14.67	16.72	16.77
	$(w_2 - w_1)/w_1$ (%)	2.49	0.29	-7.42	7.52	-0.83
	$(w_3 - w_1)/w_1$ (%)	0.86	0.37	-0.14	-0.24	-0.12
with resistance	Ma's method/w_2'	13.18	13.68	13.61	17.99	16.62
	Present method/w_3'	13.12	13.80	14.71	16.62	16.60
	$(w_2' - w_3')/w_3'$ (%)	0.46	-0.87	-7.48	8.24	0.12
$(w_3' - w_3)/w_3$ (%)		1.31	0.95	0.27	-0.60	-1.01

Table 2 Comparison of shear force of node point with existing methods /kN

Calculation methods		A	B/left	B/right	C	D/left	D/right	E
without resistance	Long's method /Q_1	0	496.9	-725.1	118.8	1064.8	-1011.2	0
	Ma's method/Q_2	0	505.7	-716.3	81.3	1032.7	-1043.3	0
	Present method/Q_3	0	499.7	-722.3	121.9	1066.5	-1009.5	0
	$(Q_2 - Q_1)/Q_1$ (%)	-	1.77	-1.21	-31.57	-3.01	3.17	-
	$(Q_3 - Q_1)/Q_1$ (%)	-	0.56	-0.39	2.78	0.17	-0.18	-
with resistance	Ma's method/Q_2'	0	506.5	-715.5	83.6	1034.6	-1041.4	0
	Present method/Q_3'	0	505.6	-716.4	134.3	1076.4	-999.6	0
	$(Q_2' - Q_3')/Q_3'$ (%)	-	0.18	-0.13	-37.75	-3.88	4.18	-
$(Q_3' - Q_3)/Q_3$ (%) (%)		-	1.18	-0.82	9.99	0.92	-0.97	-

Table 3 Comparison of node moments with existing methods /kNm

Calculation methods		A	B	C	D	E
without resistance	Long's method /M_1	0	614.9	-617.9	1705.4	-315.5
	Ma's method/M_2	0	627.8	-635.7	1495.1	-555.7
	Present method/M_3	0	461.9	-657.3	1452.5	-336.2
	$(M_2 - M_1)/M_1$ (%)	-	2.1	6.38	-12.33	76.13
	$(M_3 - M_1)/M_1$ (%)	-	24.49	10.82	-14.83	6.56
with resistance	Ma's method/M_2'	0	626.6	-629.5	1487.0	-552.3
	Present method/M_3'	0	479.3	-621.2	1400.7	-365.3
	$(M_2' - M_3')/M_3'$ (%)	-	30.73	1.34	6.16	51.2
$(M_3' - M_3)/M_3$ (%)		-	3.77	-5.49	-3.57	8.66

analysis of a line element, the element deformations and internal forces are expressed by the nodal deformations and forces. A small segmentation is needed for high calculation accuracy. If the segmentation isn't small enough, high errors will be existent in some points. However, excluding these special nodes with the some differences, when the beam-soil interface resistance is taken into account, the results derived from the present method and the results from Ma and Ai's FEM are close.

In addition, from Tables 1-3, comparing the deformations, the shear forces and the moments with and without consideration of the beam-soil interface resistance, it is found that the interface resistance has an effect on the deformation, shear force and moment of the beam. Compared with the results without consideration the beam-soil interface resistance in the current method, the maximum differences are 1.31% for the deformation, 9.99% for the shear force and 8.66% for the node moment, respectively.

6.2 Case 2

In order to have a further study about the beam-soil interface resistance effects on the behavior of foundation beam, a finite beam, as shown in Fig. 4, with length of 29.0 m, width of 3.0 m, height of 1.0 m and flexural rigidity of 5.125×10^6 kN·m^2, under a concentrated load $P_0 = 2000$ kN in the mid-span is applied to investigate the relationships of k_x~w_0, k_x~M_0, k_x~w and k_x~M. Due to the symmetric, only the right half of the beam was chosen to analysis. The geometric nonlinearity of the beam is also taken into account, namely, in the calculation $\chi = 1$.

6.2.1 Relationships among w_0, M_0 and P_0

The vertical foundation coefficient k_z is chosen as 1×10^4 kN/m^3 and the horizontal foundation coefficient k_x has two values, $k_{x1} = 0$ and $k_{x2} = k_z$. Figs. 5 and 6 illustrate the relationships among the mid-span displacement w_0, the mid-span bending moment M_0 of beam and the concentrated load P_0 with different cases.

When k_{x1} is 0, the beam-soil interface resistance is zero according to the assumption shown in the first equation in Eq. (1). Then, the problem investigated in this paper is reduced as the original elastic foundation beam problem without consideration of the beam-soil interface resistance. As shown in Figs. 5 and 6, when $k_{x1} = 0$, the mid-span deformation w_0 and the mid-span bending moment M_0 of the foundation beam increase linearly with the increase of P_0. But when $k_{x2} = k_z$, the displacements in x and z directions are coupled. And the relationships among P_0~w_0 and P_0~M_0 are non-linear with consideration of the beam-soil interface resistance.

Moreover, as shown in Figs. 5 and 6, the curves of P_0~w_0 and P_0~M_0 with consideration of the beam-soil interface resistance are both under the ones without consideration of the beam-soil interface resistance. It indicates that the beam-soil interface resistance has weakening effects on the values of the mid-span deformation and the mid-span bending moment of foundation beam.

6.2.2 Relationships among w_0, M_0, k_x and k_z

Three different vertical coefficients of the foundation reaction are chosen to analyze, they're $k_{z1}=1\times10^3$ kN/m^3, $k_{z2}=1 \times 10^4$ kN/m^3 and $k_{z3}=1 \times 10^5$ kN/m^3, respectively. Introducing the following non-dimensional parameters

$$\zeta_w = \frac{w_0}{w_{0,\max}}, \quad \zeta_M = \frac{M_0}{M_{0,\max}}$$

which denote the degrees that the weakening effect of beam-soil interface resistance on the values

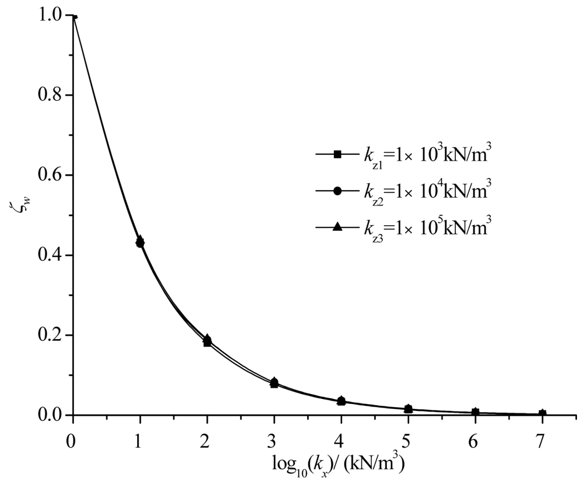

Fig. 7 Relationship between ζ_w and k_x for different k_z

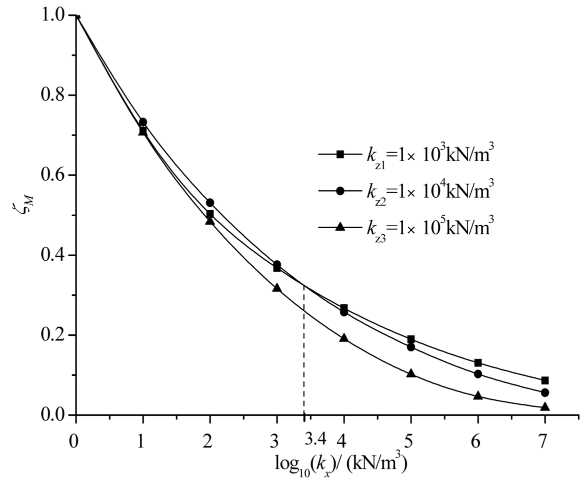

Fig. 8 Relationship between ζ_M and k_x for different k_z

of w_0 and M_0, respectively.

The variations of ζ_w and ζ_M along with the variation of the horizontal coefficient of the foundation reaction k_x are shown in Figs. 7 and 8.

From the definitions of ζ_w and ζ_M, it can be found that when ζ_w or ζ_M is smaller, the weakening effect of horizontal resistance on the values of w_0 or M_0 is larger. The maximum values of $w_{0,\max}$ and $M_{0,\max}$ in each curve in Figs. 7 and 8 are the w_0 and M_0 corresponding to $\log_{10}(k_x) = 0$ kN/m^3 (namely, $k_x = 1$ kN/m^3).

As can be seen from Figs. 7 and 8, both ζ_w and ζ_M decrease with the increase of k_x, indicating that the weakening effect of horizontal resistance on the values of w_0 and M_0 increases with the increase of the resistance value. For $k_x < 1 \times 10^{3.4}$ kN/m^3 and 1×10^3 kN/m$^3 < k_z < 1 \times 10^4$ kN/m^3, ζ_M increases with the increase of k_z, this means the effect of horizontal resistance on the value of M_0 increases with the resistance value increasing. But for $k_x < 1 \times 10^{3.4}$ kN/m^3 and 1×10^4 kN/m$^3 <$ $k_z < 1 \times 10^5$ kN/m^3 or $k_x > 1 \times 10^{3.4}$ kN/m^3, ζ_M decreases with the increase of k_z. This implies that the horizontal resistance effect on the value of M_0 decreases with the resistance value increasing. Therefore, it can be concluded that for $k_x > 1 \times 10^{3.4}$ kN/m^3, the stronger the foundation soil body is, or the rougher the interface between the beam and the foundation soil below is, or the bigger the horizontal resistance is, the greater the horizontal resistance effect on the internal force and the deflection of the foundation beam is.

6.2.3 Relationships among w_0, M_0 and k_x/k_z

The vertical foundation coefficient k_z is chosen as 1×10^4 kN/m^3 and the effect of the ratio of the horizontal foundation coefficient to the vertical one k_x/k_z on w_0 and M_0 are determined as shown in Fig. 9.

From Fig. 9, w_0 and M_0 have the same change trend with the increase of k_x/k_z, and their values both decrease with the increase of k_x/k_z. In addition, when $0 < k_x/k_z < 0.5$, the values of w_0 and M_0 decrease quickly with k_x/k_z increasing; when $0.5 < k_x/k_z < 1.25$, the values of w_0 and M_0 decrease relative slowly with k_x/k_z increasing.

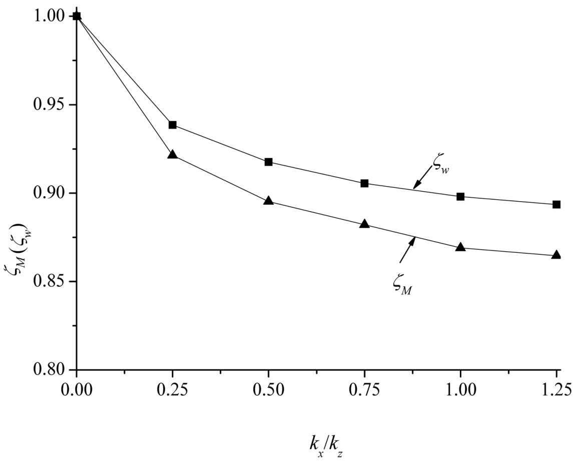

Fig. 9 Relations of ζ_w~k_x/k_v and ζ_M~k_x/k_z

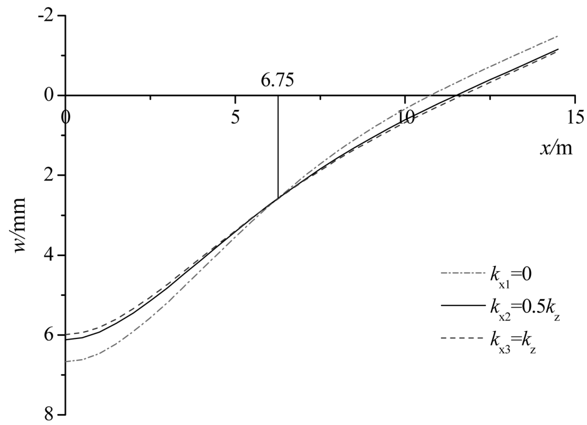

Fig. 10 Relationship between w and k_x

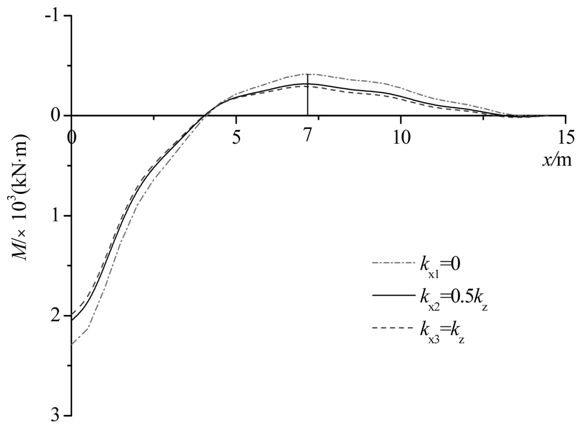

Fig. 11 Relationship between w and k_x

6.2.4 Relationship among w, M and k_x

The vertical foundation coefficient k_z is 1×10^4 kN/m^3, the horizontal foundation coefficient has three different values, $k_{x1} = 0$, $k_{x2} = 0.5k_z$ and $k_{x3} = k_z$. Figs. 10 and 11 illustrate the deflection and bending moment of foundation beam with different horizontal foundation coefficients.

As shown in Figs. 10 and 11, the horizontal foundation coefficient has a great effect on the moment and deformation of the beam. Greater the horizontal foundation coefficient is, greater the effect of the resistance between beam and the soil below on the behaviors of beam is.

7. Conclusions

In this paper, by using an iterative Galerkin method, semi analytical solutions for the deformations, axial force, shear force and bending moments of a finite beam resting on Winkler foundation have been presented with consideration of the interface resistance between beam and the foundation soil below. The coupling effect between vertical and horizontal displacements was also taken into account to obtain the solutions. A traditional Winkler elastic foundation theory and a finite element method were employed to verify the validity of the present solutions. In addition, the influences of the interface resistance on the behaviors of beam have been investigated. From the investigation, the following conclusions can be obtained:

(1) The beam-soil interface resistance has no effect on the development and change trends of bending moment and deformation of foundation beam, but has a weakening effect on their values.

(2) The larger value of the beam-soil interface resistance is, the greater weakening effect of the resistance on the internal forces and deformations of foundation beam is.

(3) The bending moment and deformation of beam decrease with increasing of k_x/k_v.

(4) It is suggested that the effect of the beam-soil interface resistance should be taken into account in engineering for economical and optimal designs, especially in the case that the contact face between the beam and the soil bed below is rough.

Acknowledgements

The research reported in this paper was funded through a project (No. 2006AA11Z104) of the High-Tech Research and Development Program of National 863 Project, China, and the Ministry of Education 985 Project.

References

Aydogan, M. (1995), "Stiffness-matrix formulation of beams with shear effect on elastic foundation", *J. Struct. Eng.*, **121**(9), 1265-1270.

Cojocaru, E.C., Irschik, H. and Schlacher, K. (2003), "Concentrations of pressure between an elastically supported beam and a moving timoshenko-beam", *J. Eng. Mech.*, **129**(9), 1076-1082.

Fabijanic, E. and Tambaca, J. (2009), "Numerical comparison of the beam model and 2D linearized elasticity", *Struct. Eng. Mech.*, **33**(5), 621-633.

Ghosh, C. and Madhav, M.R. (1994), "Reinforced granular fill-soft soil system: confinement effect", *Geotextiles and Geomembranes*, **13**(5), 727-741.

Huang, F.Y. and Shi, G.L. (1998), "Finite element analysis of pressure vessel using beam on elastic foundation analysis", *Finite Elem. Anal. Des.*, **28**, 293-302.

Hsu, M.H. (2005), "Vibration analysis of edge-cracked beam on elastic foundation with axial loading using the differential quadrature method", *Comput. Meth. Appl. Mech. Eng.*, **194**(1), 1-17.

Iimura, S. (2004), "Simplified mechanical model for evaluating stress in pipeline subject to settlement", *Construct. Build. Mater.*, **18**(6), 469-479.

Kim, N.L. (2009), "Series solutions for spatially coupled buckling analysis of thin-walled Timoshenko curved beam on elastic foundation", *Struct. Eng. Mech.*, **33**(4), 447-484.

Long, Y.Q. (1981), *Calculation of Elastic Foundation Beam*. Beijing, peoplesí education press, China. (in Chinese)

Ma, F. and Ai, Z.Y. (2002), "The finite element method of elastic subgrade beam with the contact friction effect considered", *Rock Soil Mech.*, **23**(1), 93-96. (in Chinese)

Mallik, A.K., Chandra, S. and Singh, A.B. (2006), "Steady-state response of an elastically supported infinite beam to a moving load", *J. Sound Vib.*, **291**, 1148-1169.

Onu, G. (2000), "Shear effect in beam finite element on two-parameter elastic foundation", *J. Struct. Eng.*, **126**(9), 1104-1107.

Pasternak, P.L. (1954), "On a new method of analysis of an elastic foundation by means of two foundation constants", *Gosudarstvennoe Izdatelstro Liberaturi po Stroitelsvui Arkhitekture*, Moscow, Russia.

Ruge, P. and Birk, C. (2007), "A comparison of infinite Timoshenko and Euler-Bernoulli beam models on Winkler foundation in the frequency- and time-domain", *J. Sound Vib.,* **304**, 932-947.

Sato, M., Kanie, S. and Mikami, T. (2007), "Structural modeling of beams on elastic foundations with elasticity couplings", *Mech. Res. Commun.*, **34**(5-6), 451-459.

Tan, Z.M. (1997), "The solution of elastic foundation beam considering horizontal frictional resistance", *Mech. Eng.* **19**(3), 33-35. (in Chinese)

Winkler, E. (1867), *Die Lehre von der Elastizitat and Festigkeit (On elasticity and fixity)*, H. Dominicus, Prague, Czechoslovakia.

Yin, J.H. (2000a), "Comparative modeling study of reinforced beam on elastic foundation", *J. Geotech. Geoenviron. Eng.*, **126**(3), 265-271.

Yin, J.H. (2000b), "Closed-form solution for reinforced Timoshenko beam on elastic foundation", *J. Eng. Mech.*, **126**(8), 868-874.

Zhang, L., Zhao, M.H., Zou, X.W. and Zhao, H. (2009), "Deformation analysis of geocell reinforcement using winkler model", *Comput. Geotech.*, **36**, 977-983.

Zhang, Y. and Murphy, K.D. (2004), "Response of a finite beam in contact with a tensionless foundation under symmetric and asymmetric loading", *Int. J. Solids Struct.*, **41**, 6745-6758.

Zhao, M.H., Ma, B.H. and Zhang, L. (2008a), "Fractional-step calculation method for geocell reinforced mat considering the effect of horizontal frictional resistance", Journal of Hunan University Natural Sciences, **35** (SUPPL.), 182-187. (in Chinese)

Zhao M.H., Ma, B.H. and Zhang, L. (2009a), "Fractional-step calculation method for finite length elastic foundation beam considering the effect of horizontal frictional resistance", *Eng. Mech.*, **26**(9), 16-23. (in Chinese)

Zhao, M.H., Zhang, L. and Ma, B.H. (2008b), "Force analysis of geocell reinforcement based on Winkler model", *J. Hyd. Eng.*, **39**(6), 697-702. (in Chinese)

Zhao, M.H., Zhang, L., Ma, B.H. and Zhao, H. (2009b), "Nonlinear analysis of beams on elastic foundation with consideration of horizontal resistance", *Chinese J. Geotech. Eng.*, **31**(7), 985-990. (in Chinese)

Zhao, M.H., Zhang, L., Ma, B.H. and Zhao, H. (2009c), "Nonlinear analysis of finite-length beams on Winkler foundation with horizontal resistance", *China Civil Eng. J.*, **42**(7), 106-112. (in Chinese)

Zhou, J.K. and Du, Q.Q. (2004), "Modified Winkler foundation model with horizontal force taken into account", *J. Hohai Univ.*, **32**(6), 669-673. (in Chinese)

Appendix A

In the finite element method (FEM) conducted by Ma and Ai's study (2002), the line element *ij* as shown in Fig. A.1 was employed to analysis. The displacements of the element can be expressed by

$$\begin{Bmatrix} u \\ w \end{Bmatrix} = \begin{bmatrix} N_1 & 0 & 0 & N_4 & 0 & 0 \\ 0 & N_2 & N_3 & 0 & N_5 & N_6 \end{bmatrix} \{\delta^e\} \tag{A.1}$$

where u and w are the horizontal and vertical displacements on the neutral axis of the beam, respectively; N_j ($j = 1, 2, \ldots, 6$) are the shape factors with the values: $N_1 = 1-\frac{x}{l}$; $N_2 = 1-3\frac{x^2}{l^2}+2\frac{x^3}{l^3}$; $N_3 = x-2\frac{x^2}{l}+2\frac{x^3}{l^2}$, $N_4 = \frac{x}{l}$; $N_5 = 3\frac{x^2}{l^2}-2\frac{x^3}{l^3}$; $N_6 = -\frac{x^2}{l}+\frac{x^3}{l^2}$; $\{\delta^e\}$ is the nodal deformations, $\{\delta^e\} = [u_i \ w_i \ \theta_i \ u_j \ w_j \ \theta_j]^T$; and θ is the rotation angle of the beam.

Then, the relative horizontal displacement at the beam lower side is

$$\{\Delta u\} = \left[u - \frac{h}{2}\frac{dw}{dw}\right]$$

$$= \left[N_1 \ -\frac{h}{2}\frac{dN_2}{dx} \ -\frac{h}{2}\frac{dN_3}{dx} \ N_4 \ -\frac{h}{2}\frac{dN_5}{dx} \ -\frac{h}{2}\frac{dN_6}{dx}\right]\{\delta^e\}$$

$$= [A]\{\delta^e\} \tag{A.2}$$

where $[A] = \left[N_1 \ -\frac{h}{2}\frac{dN_2}{dx} \ -\frac{h}{2}\frac{dN_3}{dx} \ N_4 \ -\frac{h}{2}\frac{dN_5}{dx} \ -\frac{h}{2}\frac{dN_6}{dx}\right]$.

Assuming the horizontal friction τ_x has a linear relationship with the horizontal displacement Δu, namely, $\tau_x = k_x \Delta u$, then

$$\{\tau_x\} = k_x(\Delta u) \tag{A.3}$$

where k_x is the horizontal coefficient of the soil reaction.

By applying the virtual work principle, the following equation is obtained

$$\{\delta^*\}^T\{F^e\} = \int_0^l \{\varepsilon^*\}^T\{\tau_x\}dx \tag{A.4}$$

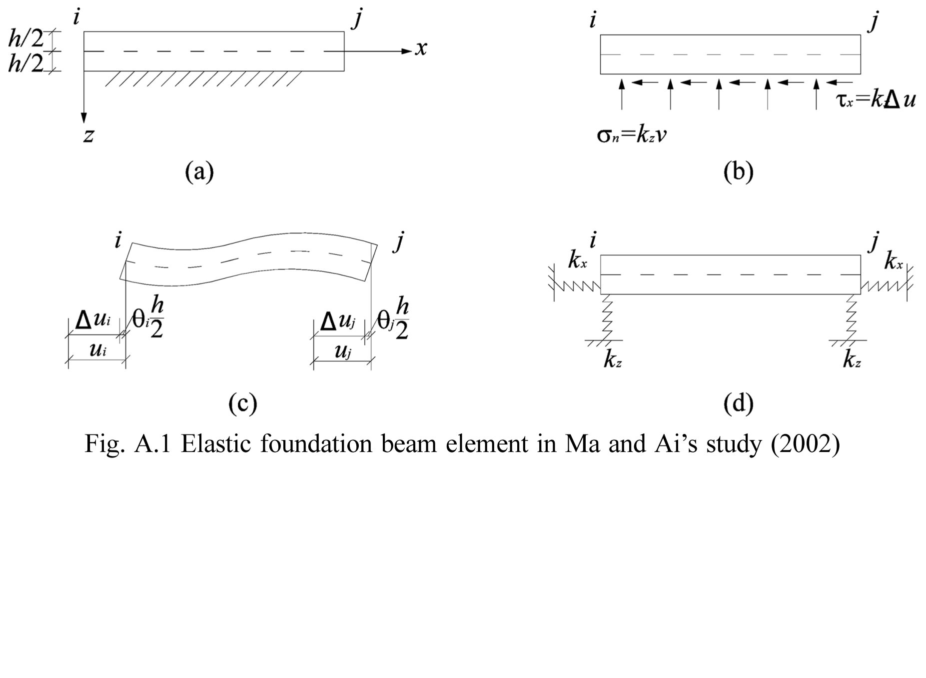

Fig. A.1 Elastic foundation beam element in Ma and Ai's study (2002) where $\{\delta^*\}$ is the virtual displacement; $\{F^e\}$ is the nodal force vector of the element *ij*, $\{F^e\} = [N_i \;\; Q_i, M_i \;\; N_j \;\; Q_j \;\; M_j]$; and $\{\varepsilon^*\}$ is the corresponding virtual strain.

Substituting $\{F^e\} = [K^e]\{\delta^e\}$ (where $[K^e]$ is the element stiffness matrix), $\{\varepsilon^*\} = [A]\{\delta^*\}$ and Eq. (A.3) into Eq. (A.4) obtains

$$\{\delta^*\}^T[K^e]\{\delta^e\} = \{\delta^*\}^T\left(\int_0^l (k_s[A]^T[A])dx\right)\{\delta^e\} \tag{A.5}$$

Then, the element stiffness matrix which considers the contact friction effect was deduced:

$$[K^e] = k_s\int_0^l ([A]^T[A])dx$$
$$= k_s\begin{bmatrix} \frac{l}{3} & \frac{h}{4} & -\frac{lh}{24} & \frac{l}{6} & -\frac{h}{4} & \frac{lh}{24} \\ \frac{h}{4} & \frac{3h^2}{10l} & \frac{h^2}{40} & \frac{h}{4} & -\frac{3h^2}{10l} & \frac{h^2}{40} \\ -\frac{lh}{24} & \frac{h^2}{40} & \frac{h^2 l}{30} & \frac{lh}{24} & -\frac{h^2}{40} & -\frac{h^2 l}{120} \\ \frac{l}{6} & \frac{h}{4} & \frac{lh}{24} & \frac{l}{3} & -\frac{h}{4} & -\frac{lh}{24} \\ -\frac{h}{4} & -\frac{3h^2}{10l} & -\frac{h^2}{40} & -\frac{h}{4} & \frac{3h^2}{10l} & -\frac{h^2}{40} \\ \frac{lh}{24} & \frac{h^2}{40} & -\frac{h^2 l}{120} & -\frac{lh}{24} & -\frac{h^2}{40} & \frac{h^2 l}{30} \end{bmatrix} \tag{A.6}$$

Adding this stiffness matrix into the common stiffness matrix, $[K_0^e]$, used in the common bar-system finite element method obtains a new stiffness matrix $[\bar{K}^e]$

$$[\bar{K}^e] = [K^e] + [K_0^e] \tag{A.7}$$

The other steps are the same as those in the common bar-system finite element method, only need to substitute $[K_0^e]$ by $[\bar{K}^e]$ in the calculation.

Appendix B

The solutions for the deformation *w*, bending moment *M* and shear force *Q* of a finite beam (Fig. B.1) derived from the classical theory for the Winkler elastic foundation beam (Long 1981) are shown as follow.

For $0 \le x \le x_1$,

$$\begin{cases} w = w_a\phi_1(\delta x) + \theta_a\frac{1}{\delta}\phi_2(\delta x) - M_a\frac{1}{EI\delta^2}\phi_3(\delta x) - Q_a\frac{1}{EI\delta^3}\phi_4(\delta x) \\ M = w_a\cdot 4EI\delta^2\phi_3(\delta x) + \theta_a\cdot 4EI\delta\phi_4(\delta x) + M_a\phi_1(\delta x) + Q_a\frac{1}{\xi}\phi_2(\delta x) \\ Q = w_a\cdot 4EI\delta^3\phi_2(\delta x) + \theta_a\cdot 4EI\delta^2\phi_3(\delta x) - M_a\cdot 4\delta\phi_4(\delta x) + Q_a\phi_1(\delta x) \end{cases}$$

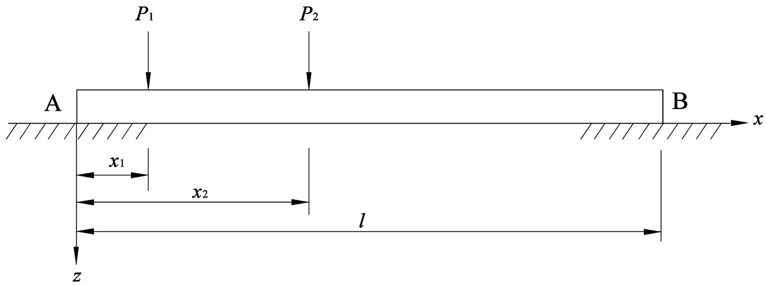

Fig. B.1 Finite beam under discretional concentrated loads

For $x_1 \le x \le x_2$,

$$\begin{cases} w = w_a\phi_1(\delta x) + \theta_a \dfrac{1}{\delta}\phi_2(\delta x) - M_a \dfrac{1}{EI\delta^2}\phi_3(\delta x) - Q_a \dfrac{1}{EI\delta^3}\phi_4(\delta x) + P_1 \dfrac{1}{EI\delta^3}\phi_4[\delta(x-x_1)] \\ M = w_a \cdot 4EI\delta^2\phi_3(\delta x) + \theta_a \cdot 4EI\delta\phi_4(\delta x) + M_a\phi_1(\delta x) + Q_a \dfrac{1}{\delta}\phi_2(\delta x) - P_1 \dfrac{1}{\delta}\phi_2[\delta(x-x_1)] \\ Q = w_a \cdot 4EI\delta^3\phi_2(\delta x) + \theta_a \cdot 4EI\delta^2\phi_3(\delta x) - M_a \cdot 4\delta\phi_4(\delta x) + Q_a\phi_1(\delta x) - P_1\phi_1[\delta(x-x_1)] \end{cases}$$

For $x_1 \le x \le l$,

$$\begin{cases} w = w_a\phi_1(\delta x) + \theta_a \dfrac{1}{\delta}\phi_2(\delta x) - M_a \dfrac{1}{EI\delta^2}\phi_3(\delta x) - Q_a \dfrac{1}{EI\delta^3}\phi_4(\delta x) + P_1 \dfrac{1}{EI\delta^3}\phi_4[\delta(x-x_1)] + P_2 \dfrac{1}{EI\delta^3}\phi_4[\delta(x-x_2)] \\ M = w_a \cdot 4EI\delta^2\phi_3(\delta x) + \theta_a \cdot 4EI\delta\phi_4(\delta x) + M_a\phi_1(\delta x) + Q_a \dfrac{1}{\delta}\phi_2(\delta x) - P_1 \dfrac{1}{\delta}\phi_2[\delta(x-x_1)] - P_2 \dfrac{1}{\delta}\phi_2[\delta(x-x_2)] \\ Q = w_a \cdot 4EI\delta^3\phi_2(\delta x) + \theta_a \cdot 4EI\delta^2\phi_3(\delta x) - M_a \cdot 4\delta\phi_4(\delta x) + Q_a\phi_1(\delta x) - P_1\phi_1[\delta(x-x_1)] - P_2\phi_1[\delta(x-x_2)] \end{cases}$$

In the above equations, w_a, θ_a, M_a and Q_a are the deformation, rotation angle, bending moment and shear force at the left end point of the beam; EI is the flexural rigidity of the beam ; $\delta = \sqrt[4]{k_v b/4EI}$; k_v is the vertical foundation coefficient; ϕ_1~ϕ_4 are Krannov functions with expressions as below

$$\begin{cases} \phi_1(\delta x) = \mathrm{ch}\delta x \cos\delta x \\ \phi_2(\delta x) = \dfrac{1}{2}(\mathrm{ch}\delta x \sin\delta x + \mathrm{sh}\delta x \cos\delta x) \\ \phi_3(\delta x) = \dfrac{1}{2}\mathrm{sh}\delta x \sin\delta x \\ \phi_4(\delta x) = \dfrac{1}{4}(\mathrm{ch}\delta x \sin\delta x - \mathrm{sh}\delta x \cos\delta x) \end{cases}$$